International Journal of Pharmaceutics 359 (2008) 247–253

Contents lists available at ScienceDirect

International Journal of Pharmaceutics

journal homepage: www.elsevier.com/locate/ijpharm

Pharmaceutical nanotechnology

Glycyrrhizin surface-modified chitosan nanoparticles for hepatocyte-targeted delivery

Aihua Lin[a,b,*], Yiming Liu[b], Yu Huang[b], Jingbo Sun[b], Zhifeng Wu[b], Xian Zhang[b], Qineng Ping[a,**]

[a] Department of Pharmaceutical Technology, Faculty of Pharmacy, China Pharmaceutical University, Nanjing, Jiangsu 210009, People's Republic of China
[b] The Second Faculty of Clinical Medicine, Guangzhou University of Traditional Chinese Medicine, Guangzhou, Guangdong 510120, People's Republic of China

ARTICLE INFO

Article history:
Received 31 October 2007
Received in revised form 23 February 2008
Accepted 23 March 2008
Available online 4 April 2008

Keywords:
Glycyrrhizin
Chitosan
Nanoparticles
Surface modification
Drug delivery
Hepatocytes

ABSTRACT

The aim of the present work was to investigate the potential utility of chitosan nanoparticles surface modified with glycyrrhizin (CS-NPs-GL) as new hepatocyte-targeted delivery vehicles. For this purpose, chitosan nanoparticles (CS-NPs) were prepared previously by ionic gelation process and glycyrrhizin was oxidized by sodium periodate to be conjugated to the surface of CS-NPs. The CS-NPs-GL obtained were first characterized for their morphology, particle size, zeta potential, association efficiency and in vitro release of adriamycin (ADR), using as a model drug. The nanoparticles were also labeled with rhodamine B isothiocyanate and their interaction with rat hepatocytes was examined by flow cytometry (FCM) and confocal laser microscopy (CLSM). The spherical nanoparticles prepared with oxidized GL/CS ratio of 0.14:1 (w/w) were in the 147.2 nm size range, and exhibited a positive electrical charge (+9.3 mV), and associated ADR quite efficiently (association efficiency: 91.7%) and showed lower extent of release (28% over 72 h) in vitro. FCM and CLSM studies showed that CS-NPs-GL were preferentially accumulated in hepatocytes and the cellular uptake amount were 4.9 times more than that in hepatic nonparenchymal cells, and the uptake process was dependent on incubation time and dose of nanoparticles, which indicated that the internalization of these nanoparticles into hepatocytes was mostly mediated by a ligand–receptor interaction. In conclusion, CS-NPs-GL as a promising hepatocyte-targeted delivery carrier holds promise for further effective studies.

1. Introduction

The development of an efficient targeted drug delivery system into cells is an important subject for the advancement of drug carriers. Active targeting has been attempted by many investigators in order to gain a high selectivity to a specific organ and to enhance the internalization of drug-loaded carriers into target cells. Receptor-mediated drug targeting is a promising approach to active targeted drug delivery. Receptor systems cannot only bind specific ligands, but can also internalize them within membrane-bond vesicles or endosomes. Once a ligand binds the receptor, the ligand–receptor complex is rapidly internalized and the receptor recycles back to the surface (Ciechanover et al., 1983). Various ligands such as folic acid and asialoglycoproteins have been introduced into drug carriers in order to enhance the intracellular localization into target cells (Stella et al., 2000; Sudimack and Lee, 2000; Maitani et al., 2001).

The liver, consisted of hepatocytes (hepatic parenchymal cells), Kupffer cells and endothelial cells (hepatic nonparenchymal cells), is an important target tissue for drug therapy, because many fatal diseases such as chronic hepatitis, enzyme deficiency and hepatoma occur in hepatocytes. However, most of particulate delivery systems are easily taken up within seconds or minutes after injection due to phagocytosis by the reticuloendothelial system (RES), including Kupffer cells of the liver and macrophages of the spleen (Redhead et al., 2001). It does represent a major barrier to deliver drugs to hepatocytes. Asialoglycoproteins receptor (ASGP-R) is well known as one of high-affinity, hepatocyte-surface receptors that can mediate drug delivery systems into hepatocytes by binding galactosyl residues (Kim et al., 2004). However, the density and activity of ASGP-R are all decreased in pathologic status and the ASGP-R mediated targeting activity to hepatocytes may be not so effective under this condition (Sawamura et al., 1984). Therefore, the discovery of new hepatocyte-specific ligands instead of using the conventional ones is very important for targeted drug delivery system into the liver.

Glycyrrhizin (GL, Fig. 1A) is one of the main compounds extracted from the root of *Glycyrrhiza glabra* (licorice). It has been proved that there are specific binding sites of glycyrrhizin on the cellular membrane of in vitro rat hepatocytes (Negishi et al., 1991;

* Corresponding author at: Department of Pharmaceutical Technology, Faculty of Pharmacy, China Pharmaceutical University, Nanjing, Jiangsu 210009, People's Republic of China. Tel.: +86 20 89091670x37403; fax: +86 20 81867705.
** Corresponding author. Tel.: +86 25 83271098; fax: +86 25 83301606.
E-mail addresses: Linah76@163.com (A. Lin), pingqn@cpu.edu.cn (Q. Ping).

0378-5173/$ – see front matter © 2008 Elsevier B.V. All rights reserved.
doi:10.1016/j.ijpharm.2008.03.039

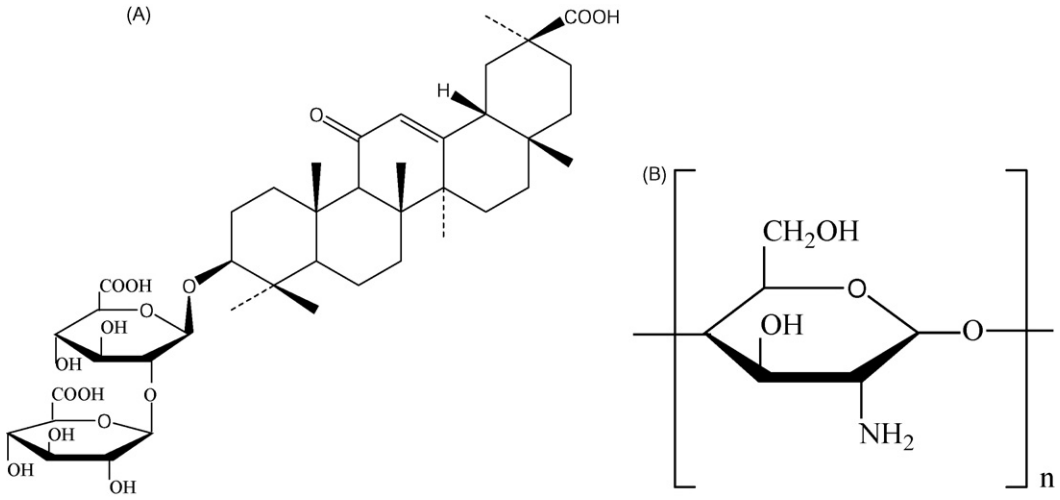

Fig. 1. Chemical structures of glycyrrhizin (A) and chitosan (B).

Ishida et al., 1993). Following intravenous administration, glycyrrhizin is rapidly cleared from the circulation by saturable uptake into the rat liver (Ishida et al., 1994). In recent years, Ismair et al. (2003) have found that carrier-mediated transport system participates in the uptake of glycyrrhizin into rat and human hepatocytes. Based on these researches, some new drug carriers surface modified with glycyrrhizin (such as liposomes and albumin nanoparticles) were prepared and proved to be more efficient on hepatocyte-targeted delivery compared with the conventional ones (Tsuji et al., 1991; Osaka et al., 1994; Mao et al., 2005). These results imply that glycyrrhizin may be used as a novel ligand for hepatocyte-specific delivery.

Recently, polymeric nanoparticles have been widely studied as carriers for drug delivery. Natural chitosan (Fig. 1B) is a cationic polysaccharide obtained by partial deacetylation of chitin, the major component of crustacean shells. Chitosan nanoparticles (CS-NPs) have a special role in drug delivery due to its biocompatibility, biodegradability, increased transfection efficiency and low toxicity (Aspden et al., 1997; Mao et al., 2001; Aktas et al., 2005). CS-NPs are usually prepared by ionic gelation based on the interaction between the negative groups of pentasodium tripolyphosphate (TPP) and the positively charged amino groups of chitosan. In our past investigation, CS-NPs prepared by this process have been proved to remain a part of free amino groups on their surface, and their properties have correlation with these residual amino groups (Lin et al., 2007).

CS-NPs with residual amino groups on the surface offer the opportunity to attach ligands binding by surface-modification. The objective of the present work was to develop a new hepatocyte-specific drug delivery system on the basis of CS-NPs and glycyrrhizin, and to evaluate its potential for hepatocyte targeting. For this purpose, glycyrrhizin surface-modified CS-NPs (CS-NPs-GL) were prepared, and their physicochemical characteristics in comparison to unmodified CS-NPs were determined within this study. Finally, The nanoparticles were labeled with rhodamine B isothiocyanate and their interaction with primary rat hepatocytes was investigated by flow cytometry (FCM) and confocal laser microscopy (CLSM).

2. Materials and methods

2.1. Materials and animals

Chitosan (deacetylation degree >85%), glycrryhizin, poly (vinyl sulfate kalium salt) (PVSK) and rhodamine B isothiocyanate (RBITC) were purchased from Sigma (St. Louis, MO, USA). Pentasodium tripolyphosphate was supplied by Tianjin Chemical Company (Tianjin, China). Adriamycin·(ADR) HCl was obtained from Haizhen Pharmaceutical Limited Company (Zhejiang, China). Toluidine blue and sodium periodate were purchased from Shanghai Chemical Reagent Limited Company (Shanghai, China). Methanol and acetonitrile were chromatographic pure. All other chemicals used were analytical pure.

Wistar rats (200 ± 20 g), from the Central Animal House of the Guangzhou University of Traditional Chinese Medicine (China), were used. They were kept in a 12 h light–dark cycle and at a temperature of 20 ± 2 °C. The animals were allowed access to food and water ad libitum.

2.2. Preparation of GL surface-modified chitosan nanoparticles

GL (0.5 μM) was dissolved in 5 ml of carbonate buffer solution (pH 9.5, 4 °C, 1.3 ml of 0.2 mol/l Na_2CO_3 with 3.7 ml of 0.2 mol/l $NaHCO_3$). It was mixed with an equal volume of cold sodium periodate solution (0.5 μM, 4 °C), and kept on ice for 90 min under magnetic stirring, then 40 ml of methanol was added to remove the sediment, and the filter liquor was carried out at 50 °C under a nitrogen stream and magnetic stirring to evaporate methanol. Next, the oxidized GL was lyophilized by a freeze dryer (Alpha1-2, Christ, Germany) to obtain the dried oxidized GL.

According to the procedure previously developed by our group (Lin et al., 2007), CS-NPs were formed spontaneously upon addition of an aqueous TPP solution (1.5 mg/ml) to CS solution (2 mg/ml, dissolved in 1% acetic solution) at volume ratio of 2:5 under magnetic stirring. ADR-loaded nanoparticles were formed upon incorporated of TPP solution into CS solution containing 0.4 mg/ml ADR at the same ratio. The pH values of the nanoparticles suspension were adjusted to about 6.0 with NaOH, and oxidized GL solution (0.5, 1 and 2 mg/ml, dissolved in distilled water) was added dropwise into the nanoparticles suspension at oxidized GL/CS ratios of 0.07:1, 0.14:1 and 0.28:1 (w/w) under magnetic stirring for 6 h, respectively. Then, the mixture was dispersed by ultrasonication for 60 s. The final volume of the mixture in each preparation was limited to 20 ml in order to yield uniform CS concentration.

2.3. Colloidal titration

The residual cationic amino groups on the surface of nanoparticles were determined by colloidal titration base on the

reaction between positively charged polyelectrolytes and negatively charged ones (Kwon et al., 2003). 5 ml of CS solution or nanoparticle suspension (5 mg of CS) mixed with 1 ml of 1% acetic solution and 100 μl of 0.2% T.B indicator, was titrated with 0.2 mmol/l PVSK standard solution until reaching the color transition, which was from blue to prunosus and hold prunosus within 10 s. Another 5 ml of double distilled water was taken to make blank assay. The amount of amino groups was calculated from the net consumed volume of PVSK standard solution (an average of at least three titrations) using the following equation (Musyanovych et al., 2007):

$$[\text{amino groups/g CS}] = \frac{\Delta V M N_A}{SC} \quad (1)$$

where ΔV is the net consumed volume of PVSK in l, M is the molar concentration of PVSK in mol/l, N_A is Avogadro's constant (6.022×10^{23} mol/l) and SC is the solid content of CS in g.

The ratio of residual amino groups (RRAGs) on the surface of nanoparticles was calculated with the following equation:

$$\text{RRAG} = \frac{\text{residual amino groups/g CS}}{\text{total amino groups/g CS}} 100. \quad (2)$$

Because M, N_A and SC of (1) equation were invariably values in this titration assay, RRAG of (2) equation was calculated with the following equation:

$$\text{RRAG} = \frac{\Delta V_1}{\Delta V_0} 100 \quad (3)$$

where ΔV_0 was the net consumed volume of PVSK standard solution in the titration of CS solution, and ΔV_1 was the net consumed volume of PVSK standard solution in the titration of nanoparticles.

2.4. Measurement of particles size and zeta potential

The particle size and zeta potential of nanoparticles were assessed, respectively, by dynamic light scattering (DLS) and laser Doppler anemometry (LDA) using a Zetasizer 3000 (Malvern Instruments, UK). The nanoparticle suspension was filtered with a 0.45 μm filter and each batch was analyzed in triplicate.

2.5. Transmission electron microscopy (TEM)

The morphology of CS-NPs or CS-NPs-GL was observed using TEM (JEM-2010HR, JEOL, Japan). One drop of nanoparticle suspension was placed on a copper grid and stained with 2% phosphotungstic acid solution for 2 min. The grid was allowed to dry at room temperature and was examined with the electron microscope.

2.6. FT-IR spectrum analysis

FT-IR spectra were measured by Avatar360 IR Spectrophotometer (Nicolet Company, USA) to determine the complex formation between oxidized GL and CS-NPs. The CS-NPs and CS-NPs-GL were separated from suspension and lyophilized by a freeze dryer. These dried nanoparticles were mixed with KBr and pressed to a plate for measurement.

2.7. Drug encapsulation and ADR measurement

The ADR-loaded nanoparticles were separated from the aqueous medium by ultrafiltration (3000 MW, Sartorius, Germany) at 3000 rpm for 15 min. The amount of free ADR in the centrifugate was measured by HPLC. 10 μl of centrifugate was injected into a chromatogram (Waters 600, Waters, American) equipped with a UV detector (Waters 996, American) and reversed phase column (ZORBAX C_8, 5 μm, 4.3 mm × 150 mm, Agillent). The mobile phase was a mixture of methanol:acetonitrile: 0.01 mol/l sodium acetate solution:glacial acetic acid = 40:10:50:1. The flow rate was 1.0 ml/min at 25 °C, and the wavelength was set at 254 nm. All measurements were performed in triplicate.

The ADR association efficiency (AE) were calculated according the following equation:

$$\text{AE} = \frac{\text{total ADR-free ADR}}{\text{total ADR}} 100.$$

2.8. In vitro release studies

In vitro ADR release profiles of nanoparticles were determined as follows. 4 ml of nanoparticles suspension was transferred to a dialysis membrane bag with a molecular cut-off of 10 kDa, tied and placed into 50 ml of PBS. The entire system was kept at 37 °C through continuous shaking bath. At appropriate time intervals, 1 ml of the release medium was removed and 1 ml fresh medium PBS solution was added into the system. The amount of ADR in the release medium was evaluated by HPLC. All measurements were performed in triplicate. The calibration curve obtained from the HPLC method was linear between 0.63 and 20 μg/ml ($C = 4.2634 \times 10^{-5} A + 0.0138$, $r = 0.9999$).

2.9. Isolation of hepatic cells and primary cultures of rat hepatocytes

Hepatic cells were isolated from the normal liver of male Wister rats (200 ± 20 g) using the in situ perfusion method (Nguyen et al., 2003). Briefly, the liver was perfused in situ through the portal vein with a 1 mg/ml collagenase type IV solution. The liver was then carefully removed and dissected, and the cells were dispersed in cold PBS solution through 300-mesh cell sieve to obtain a suspension of single cells. Differential centrifugations were used to separate parenchymal hepatocytes from hepatic nonparenchymal cells, utilizing the difference in sizes of these cells. Hepatocytes from total cells were sedimented by centrifugation at 500 rpm for 10 min and the pellet was washed three times in DEME (Gibco BRL, Paris, France) and resuspended in DEME supplemented with 10% heat inactivated fetal bovine serum, 100 units/ml penicillin, and 100 mg/ml streptomycin. Viability of hepatocytes was assessed by trypan blue exclusion immediately after isolation and was >85%. When nonparenchymal cells were needed, the supernatants were centrifuged twice (10 min at 500 rpm) to eliminate remaining hepatocytes and nonparenchymal cells were separated by centrifugation at 2000 rpm for 10 min. Finally, nonparenchymalcells were washed three times in DEME. The isolated hepatocytes were plated at a density of 2×10^6 cell/ml in six-well tissue culture dishes, and cultured at 37 °C under a humidified 5% CO_2 atmosphere for 4 h to allow them to adhere to the dish. Dead non-adhering cells were removed when the culture medium was changed for using in the following experiment.

2.10. RBITC labeling of chitosan

The synthesis of BRITC-labeled chitosan was based on the reaction between the isothiocyanate group of BRITC and the primary amino group of chitosan (Onishi and Machida, 1999; Meng et al., 2006). In this study, 100 μl of RBITC (1 mg/ml, dissolved in DMSO) was added to 100 ml of 1% chitosan solution (pH 8.5 with NaOH), and allowed to stand for 1 h at room temperature under magnetic stirring, and then added to an excess of ethanol to precipitate the RBITC-labeled chitosan. The labeled chitosan was dissolved in

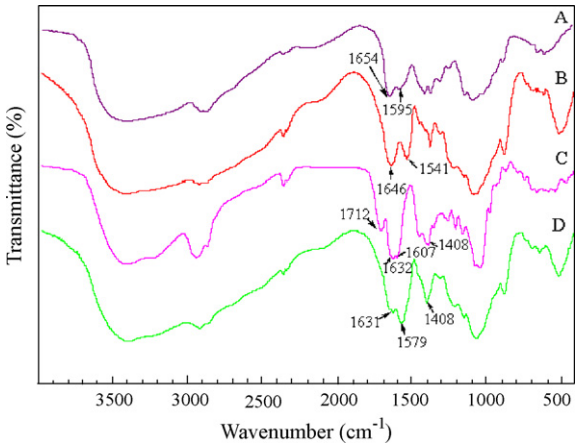

Fig. 2. FT-IR spectra of CS (A), CS-NPs (B), oxidized GL (C) and CS-NPs-GL prepared with the oxidized GL/CS ratio of 0.28:1 (w/w) (D).

100 ml of 1% acetic acid solution and dialyzed against distilled water for 3 days to remove the free RBITC. The final RBITC-labeled chitosan was obtained by freeze-drying. The nanoparticles with labeled chitosan were prepared using the same procedure as described in Section 2.2 item.

2.11. In vitro cellular uptake

To study cellular selective uptake in hepatocytes and hepatic nonparenchymal cells, hpatocytes (parenchymal cells) and nonparenchymal cells were incubated with 150 μg/ml NPs labeled with RBITC for 30 min, respectively. To study the effect of different concentration of NPs and incubation time on cellular uptake, the hepatocytes were incubated with a series of doses of NPs suspension (25, 50, 150, 300 and 500 μg/ml) for 1 h or incubated in culture medium including 150 μg/ml NPs for different incubation times (from 5 min to 24 h). The cells were then washed three times with PBS, and resuspended in fresh culture medium and placed in an incubator for 30 min to allow the cell membrane to recover. After washing twice with cold PBS, cells were transferred into tubes and immediately placed on ice. The intracellular fluorescence intensity was determined on a Beckman Coulter EPICS XL-ELITE flow cytometry (Beckman Coulter Limited, Buckinghamshire, UK) using XL EXPO^{TM} 2.0 software. Approximately 5000 event cells were evaluated to determine the trend of RBITC-labeled NPs taken up by cells. All samples were repeated three times.

Table 1
The effect of the ratio of oxidized GL/CS on RRAG, particle size and zeta potential of nanoparticles (mean ± S.D., $n = 3$)

The ratio of oxidized GL/CS (w/w)	RRAG (%)[a]	Particle size (nm)	Zeta potential (mV)
0	41.2 ± 0.6	247.5 ± 28.3	34.5 ± 1.7
0.07:1	35.2 ± 0.9	206.7 ± 13.6	10.8 ± 0.7
0.14:1	25.3 ± 1.1	147.2 ± 17.9	9.3 ± 0.5
0.28:1	10.8 ± 0.8	257.8 ± 21.2	6.2 ± 0.8

[a] The ratio of residual amino groups (RRAG) in the CS solution was set to 100%.

2.12. Confocal laser scanning microscopy (CLSM)

For CLSM studies, the hepatocytes were incubated with 150 μg/ml NPs labeled with RBITC for 30 min or 3 h. The cells were subsequently washed three times with cold PBS, and visualized and imaged under a Leica TCS SP3 confocal microscopy (Leica, Heidelberg, Germany) with filter at 543 nm.

3. Results and discussion

3.1. Surface conjugation of GL

Two steps were taken to conjugate GL to the surface of CS nanoparticles in the present study. The first step consisted of introducing aldehyde groups to GL, which contains two glucuronic acids that possess the adjacent hydroxyls structure, by periodate oxidation (Mao et al., 2003). In the second step, the modified GL was then reacted with residual amino groups on the surface of CS-NPs. The nanoparticles were obtained by these procedures under very mild conditions without the need of high temperature, organic solvent, surfactant and some other special experimental technology.

Fig. 2 shows the FT-IR spectra of CS, CS-NPs, oxidized GL and CS-NPs-GL prepared with oxidized GL/CS ratio of 0.28:1 (w/w). For CS-NPs (Fig. 2B), changes in the amine absorption bands were detected. These spectral changes were attributed to the electrostatic interaction between CS amine and TPP phosphoric groups (Wu et al., 2005; Tiyaboonchai and Limpeanchob, 2007). Electrostatic interaction with CS amine made these groups absorption band shift from 1654 cm^{-1} of amide band I and 1595 cm^{-1} of amide band II in pure CS (Fig. 2A) to 1646 cm^{-1} and 1541 cm^{-1}, respectively. In the spectrum of CS-NPs-GL (Fig. 2D), the intensities of amine groups absorption decreased dramatically, and new strong absorption bands at 1579 cm^{-1} was observed, which suggest that the interaction between oxidized GL and CS-NPs generates new

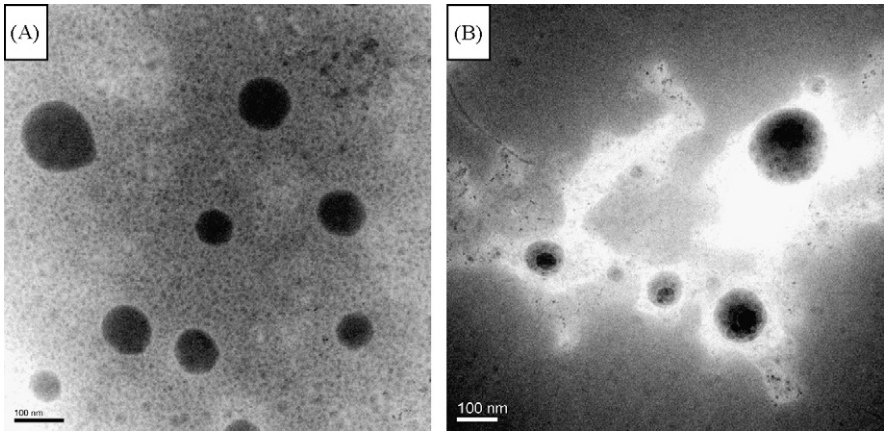

Fig. 3. Transmission electron micrographs of CS-NPs (A) and CS-NPs-GL prepared with the oxidized GL/CS ratio of 0.14:1 (w/w) (B).

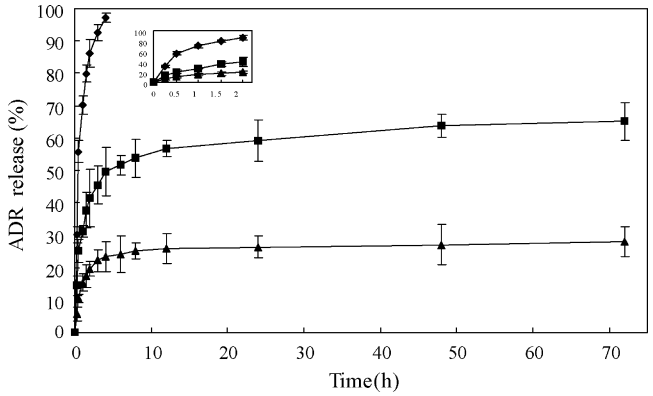

Fig. 4. In vitro ADR release profiles of nanoparicles in PBS at 37 °C, equal volumes of nanoparticles suspension and free ADR·HCl solution were put into a dialysis bag, and then dialyzed against release medium under dark condition. (▲) CS-NPs-GL; (■) unmodified CS-NPs; (♦) free ADR solution. Mean ± S.D. (n = 3).

C=N bonds of Schiff's base. Furthermore, the absorption peak of carboxyl groups stretching vibration (at 1731 cm^{-1} in oxidized GL (Fig. 2C)) disappeared, and 1408 cm^{-1} of COO^- symmetric stretching vibration appeared. The peak of COO^- asymmetric stretching vibration at 1607 cm^{-1} might be stacked in the absorption peaks at 1571 cm^{-1} (Hu et al., 2002), and the absorption peaks at 1631 cm^{-1} was assigned to vibrations of conjugated double bond, which could be observed at 1632 cm^{-1} in oxidized GL. These results indicate that not only chemical interaction occurs between oxidized GL and CS-NPs, but also the carboxyl groups of oxidized GL are dissociated into COO^- anion groups, which were bound to protonated residual amino groups of CS nanoparticles through electrostatic interaction to form CS-NPs-GL.

3.2. Particle characterization

It was believed that the preparation of chitosan nanoparticles by ionic gelation could decrease the amount of primary amino groups of chitosan. In this study, the quantification of these groups was performed with PVSK standard solution. The ratio of residual amino groups on the surface of nanoparticles, particle size and zeta potential of nanoparticles prepared with different proportions of oxidized GL/CS are presented in Table 1. The results were demonstrated that 41.2% of RRAG on the particle surface were sufficiently available for GL conjugation. With increasing proportion of oxidized GL/CS, decreased RRAG proved that GL was conjugated to amino groups on the surface of CS-NPs, and complex formation led to decrease ionizable amino groups ($-NH_3^+$) density of nanoparticles, which was in agreement with the FT-IR spectra results above. It is also interesting to find that the mean diameters of particles decreased at first, and then increased with proportion of oxidized GL/CS. These can be explained by the presence of intra- and inter-molecular linkages occurred between oxidized GL and amino groups on the surface of CS-NPs. At low ratio of oxidized GL/CS, the diameter of nanogels showed a tendency to diminish due to the intra-molecular linkages, resulting in the formation of compact solid matrix structure. As the amount of oxidized GL in the system increased, the interactions between oxidized GL and amino groups were affected not only by intra-molecular but also inter-molecular linkages, resulting in a continuous increase of the diameter (Lopez-Leon et al., 2005). $-NH_3^+$ density on the surface of nanoparticles was responsible for the measured positive zeta potential values obtained for all formulations. Positive zeta potential of nanoparticles stepped down as decreased $-NH_3^+$ density, indicating that the system would easily lose its colloidal stability at high ratio of oxidized GL/CS. In this study, CS-NPs-GL prepared with the oxidized GL/CS ratio exceeding 0.54:1 were to aggregate (data not shown). Carrier systems with diameters larger than 200 nm are known to induce nonspecific scavenging by monocytes and the reticuloendothelial system (Gabizon et al., 1990; Na et al., 2003). The nanoparticles obtained with the oxidized GL/CS ratio of 0.14:1 were within 200 nm size ranges, and exhibited a positive electrical charge (+9.3 mV), which could be suitable for the following studies.

The morphological characteristic of nanoparticles is shown in Fig. 3. The CS-NPs (Fig. 3A) exhibit solid and consistent spherical shapes, and the CS-NPs-GL (Fig. 3B) exhibit compact cores

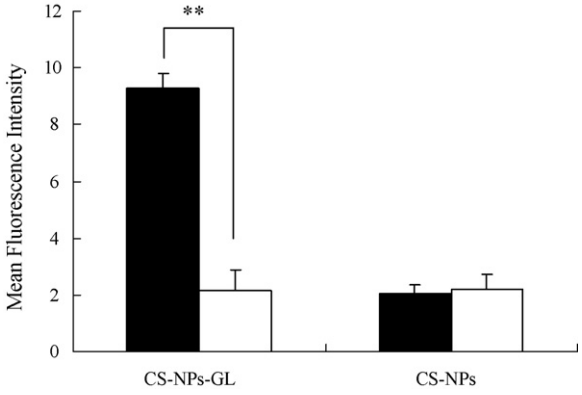

Fig. 5. Hepatic cellular selective uptake of CS-NPs-GL and unmodified CS-NPs (150 μg) between primary rat hepatocytes (■) and nonparenchymal cells (□). Mean fluorescence intensity (MFI) was determined after 30 min co-incubation. Mean ± S.D. (n = 3); $^{**}p < 0.001$.

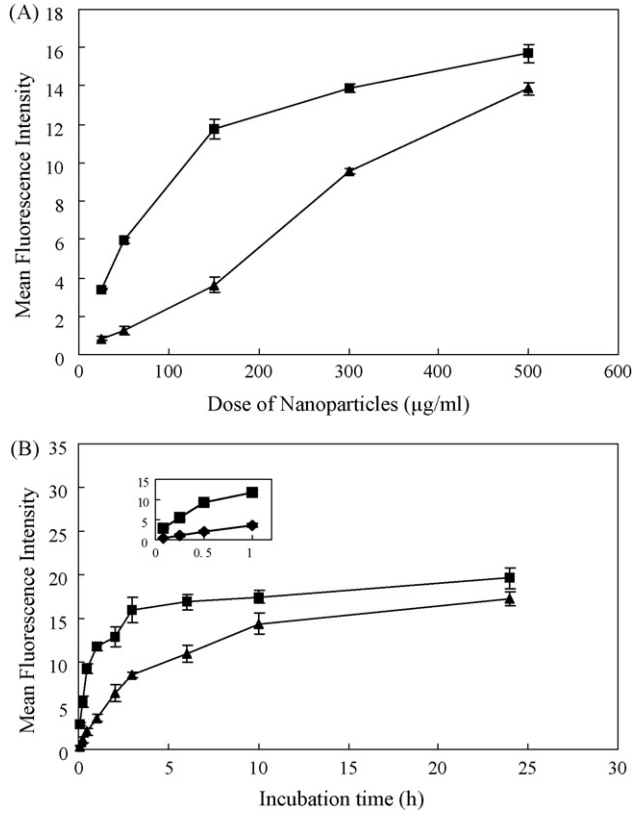

Fig. 6. The cellular level of mean fluorescence intensity (MFI) at (A) different nanoparticle concentrations after 1 h co-incubation and (B) different incubation time with 150 μg of nanopaticles. (■) CS-NPs-GL; (▲) unmodified CS-NPs. Mean ± S.D. (n = 3).

surrounded by complex coacervate. In the process of dropping oxidized GL into CS-NPs suspension, the CS-NPs could be deswollen and form compact inner-cores at the early stage of the formulation of CS-NPs-GL, then GL/CS complex coacervate layers were formed on the surface of inner-cores through covalent and electrostatic interaction. Because these nanoparticles were dried to the TEM characterization, the size of estimated from TEM (<100 nm) is smaller than that determined by DLS (>140 nm, as seen in Table 1) in water, which swelled chitosan nanogel particles.

3.3. ADR encapsulation and release test

In order to investigate the feasibility of using CS-NPs-GL as a hepatocyte-targeted drug carrier, ADR as a model drug was loaded into CS-NPs-GL prepared with the oxidized GL/CS ratio of 0.14:1. ADR encapsulation efficiencies of CS-NPs and CS-NPs-GL were 65.5% ± 2.1% and 91.7% ± 3.2%, respectively. The reason for the increased encapsulation efficiency of CS-CS-GL may be due to molecular structure of ADR·HCl, containing ionizable groups. The electrostatic interactions between negative groups of oxidized GL and the positive groups of ADR·HCl may play a role in association of more amount of free ADR·HCl from CS solution to nanoparticles.

Fig. 4 displayed the release profiles of ADR from nanoparticles in PBS. In this study, the free ADR solution was used as control to reflect the diffusion rate of ADR through the dialysis membrane bag. It was observed that 97.2% of ADR diffused into PBS in 4 h. The total amounts of drug released from the CS-NPs and CS-NPs-GL over 72 h were nearly 70% and 28%, respectively. It was apparent from the results that ADR release rate from CS-NPs-GL in vitro was fairly slower in comparison to unmodified CS-NPs under the same condition. This may be explained by a possible complex formation between polymer matrix and the entire amount of ADR loaded. ADR could be associated to the nanoparticles in three different states: (a) at the nanoparticle surface, (b) in the core as a reversible complex with polymer matrix, or (c) in the core as an irreversible complex with polymer matrix. The burst release of drug loaded in CS-NPs (25% in 30 min) is associated with those drug molecules dispersing close to the nanoparticle surface, which easily diffuse in the initial incubation time. GL/CS complex coacervate layer on the surface of CS-NPs-GL made the release medium more difficultly to access to the core of the nanoparticles, and ADR was expected to dissolve and diffuse more slowly to the outer aqueous phase relative to a molecular dispersion, which lead to lower extent of release.

3.4. Cellular selective uptake of nanoparticles

Fluorescently labeled nanoparticles can provide a rapid, simple and sensitive means to quantify cell-associated nanoparticles. In this study, CS was labeled with RBITC as a fluorescence probe to observe the interaction between nanoparticles and hepatic cells. Fig. 5 shows the cellular selective uptake of CS-NPs-GL and CS-NPs in hepatocytes and nonparenchymal cells of the liver after 30 min incubation. We found that CS-NPs-GL were significantly accumulated in hepatocytes ($p < 0.001$), and the uptake amount of CS-NPs-GL in hepatocytes were 4.9 times more than that in nonparenchymal cells, while CS-NPs showed similar uptake levels in both cell types. From this result it appears that GL plays a major role in hepatocyte-selective uptake of these nanoparticles and indicated that the increased uptake of CS-NPs-GL is resulted from efficient recognition by the GL receptor on hepatocytes.

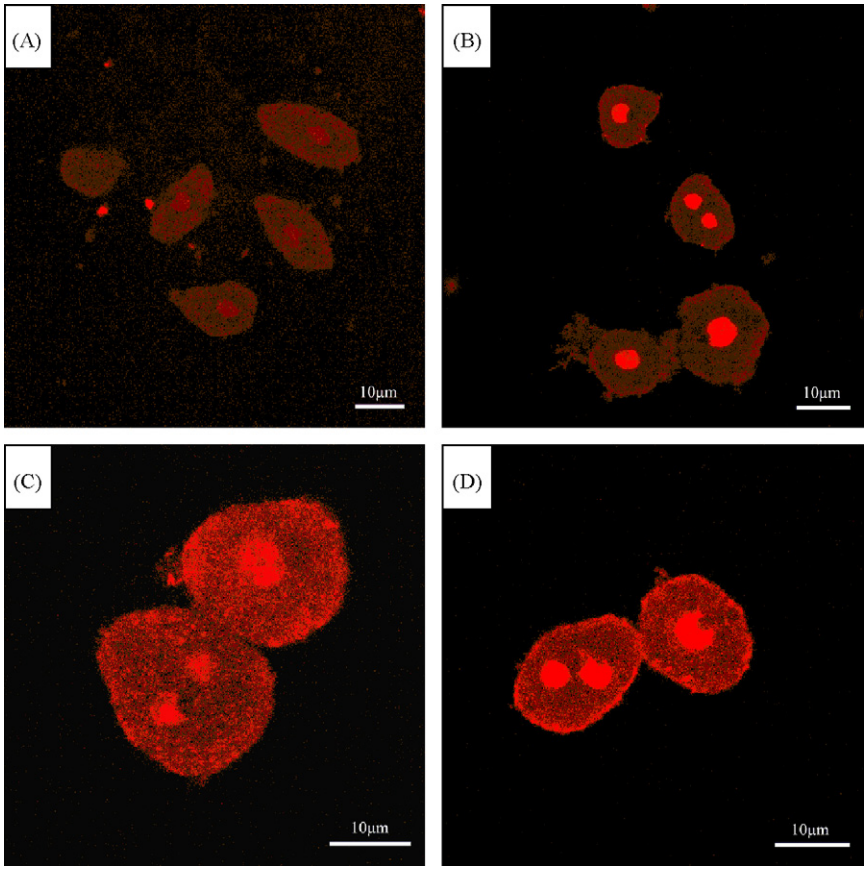

Fig. 7. Confocal laser scanning microscope (CLSM) images of the primary rat hepatocytes treated with unmodified CS-NPs and CS-NPs-GL (150 μg) after 30 min and 3 h co-incubation. (A) Cells were incubated with CS-NPs for 30 min; (B) cells were incubated with CS-NPs-GL for 30 min; (C) cells were incubated with CS-NPs for 3 h; (D) cells were incubated with CS-NPs-GL for 3 h; scale bar: 10 μm.

3.5. Observation of the nanoparticle uptake into hepatocytes

As shown in Fig. 6A, the cellular level of mean fluorescence intensity (MFI) increased obviously with dose of CS-NPs-GL at low concentrations, and the process seemed saturable at high concentrations. However, the uptake of the control CS-NPs increased linearly. The result indicated that the cellular uptake of CS-NPs-GL was dose dependant. Fig. 6B shows the cellular uptake for different co-incubation time using rat hepatocytes treated with 150 μg/ml of the nanoparticles. The MFI of CS-NPs-GL increased sharply within initial 2 h of incubation time, indicating that receptor-mediated endocytosis is initiated by ligand binding to hepatocyte membrane receptors. Whereas, the uptake of CS-NPs increased progressively with incubation time, indicating that passively adsorptive endocytosis is exhibited simultaneously by nonspecific interaction of the cell membrane (Huang et al., 2002). Confocal imaging of primary rat hepatocytes after uptake experiments supported the quantitative data generated from the FCM studies. Fig. 7 clearly shows the nanoparticle uptake by hepatocytes were internalized into cytoplasm and enriched in nucleus. Cells incubated with CS-NPs-GL exhibited stronger fluorescence than cells incubated under the same conditions with CS-NPs after 30 min and 3 h co-incubation. However, there was no apparent difference in subcellular localization shown by these two groups of cells, indicating that the GL surface-modification does not affect the characterization of intracellular distribution of CS-NPs. As stated above, a higher intracelluar content of a drug via endocytosis of a carrier may remarkably increase the therapeutic effect against the target cells (Meschini et al., 1994). The excessive uptake of CS-NPs-GL by hepatocytes compared with the control CS-NPs could hold promise for the specific receptor-mediated cellular endocytosis of these nanoparticles.

4. Conclusions

CS-NPs-GL have been prepared in order to develop a drug delivery system targeted the liver by the specific interaction between GL and hepatocytes. All these CS-NPs-GL are obtained under mild conditions without any organic solvents and surfactants, which are more suitable for pharmaceutical applications. The ratio of oxidized GL/CS has a great influence on the properties of CS-NPs-GL. The results of model drug (ADR) loading and release experiments indicate that this system seems to be a very promising vehicle for encapsulation of ionizable drugs under acidic or neutral conditions. FCM and CLSM studies show that CS-NPs-GL are preferentially accumulated in hepatocytes and the cellular uptake of CS-NPs-GL is dependent on the incubation time and dose of nanoparticles, which indicates that this process is mostly mediated by a ligand–receptor interaction. This work can be considered as the first step for further study on the application of CS-NPs-GL as a promising carrier for possible drug delivery targeted the liver in vivo.

Acknowledgement

This study was supported by the Natural Science Foundation of Guangdong Province, China (No.04010047).

References

Aktas, Y., Andrieux, K., Alonso, M.J., Calvo, P., Gürsoy, R.N., Couvreur, P., Capan, Y., 2005. Preparation and in vitro evaluation of chitosan nanoparticles containing a caspase inhibitor. Int. J. Pharm. 298, 378–383.

Aspden, T.J., Mason, J.D., Jones, N.S., Lowe, J., Skaugrud, O., Illum, L., 1997. Chitosan as a nasal delivery system: the effect of chitosan colutions on in vitro and in vivo mucociliary transport rates in human turbinates and volunteers. J. Pharm. Sci. 4, 509–513.

Ciechanover, A., Schwartz, A.L., Lodish, H.F., 1983. Sortion and recycling of cell surface receptors and endocytosed ligands: the asialoglycoprotein and transferrin receptors. J. Cell Biochem. 23, 107–130.

Gabizon, A., Price, D.C., Hberty, J., Bresalier, R.S., Papahadjiopoulos, D., 1990. Effect of liposome composition and other factors on the targeting of liposomes to experimental tumors: biodistribution and imaging studies. Cancer Res. 50, 6371–6378.

Hu, Y., Jiang, X.Q., Ding, Y., Ge, H.X., Yuan, Y.Y., Yang, C.Z., 2002. Synthesis and characterization of chitosan-ploy(acrylic acid) nanoparticles. Biomaterials 23, 3193–3201.

Huang, M., Ma, Z.S., Khor, E., Lim, L.Y., 2002. Uptake of FITC-chitosan nanoparticles by A549 cells. Pharm. Res. 19, 1488–1494.

Ishida, S., Sakiya, Y., Ichikawa, T., Taira, Z., 1993. Uptake of glycyrrhizin by isolated rat hepatocytes. Biol. Pharm. Bull. 16, 293–297.

Ishida, S., Sakiya, Y., Taira, Z., 1994. Disposition of glycyrrhizin in the perfused liver of rats. Biol. Pharm. Bull. 17, 960–969.

Ismair, M.G., Stanca, C., Ha, H.R., Renner, E.L., Meier, P.J., Kullak-Ublick, G.A., 2003. Interactions of glycyrrhizin with organic anion transporting polypeptides of rat and human liver. Hepatol. Res. 26, 343–347.

Kim, T.H., Park, I.K., Nah, J.W., Choi, Y.J., Cho, C.S., 2004. Galactosylated chitosan/DNA nanoparticles prepared using water-soluble chitosan as a gene carrier. Biomaterials 25, 3783–3792.

Kwon, S., Park, J.H., Chung, H., Kwon, I.C., Jeong, S.Y., 2003. Physicochemical characteristics of self-assembled nanoparticles based on glycol chitosan bearing 5 h-cholanic acid. Langmuir 19, 10188–10193.

Lin, A.H., Liu, Y.M., Ping, Q.N., 2007. Studies of free amino groups on the surface of chitosan nanoparticles and its characteristics. Yao Xue Xue Bao 42, 323–328.

Lopez-Leon, T., Carvalho, E.L., Seijo, B., Ortega-Vinuesa, J.L., Bastos-González, D., 2005. Physicochemical characterization of chitosan nanoparticles: electrokinetic and stability behavior. J. Colloid Interface Sci. 283, 344–351.

Maitani, Y., Kawano, K., Yamada, K., Nagai, T., Takayama, K., 2001. Efficiency of liposomes surface-modified with soybean-derived sterylglucoside as a liver targeting carrier in HepG2 cells. J. Control. Release 75, 381–389.

Mao, H.Q., Roy, K., Troung-Le, V.L., Janes, K.A., Lin, K.Y., Wang, Y., August, J.T., Leong, K.W., 2001. Chitosan–DNA nanoparticles as gene carriers: synthesis, characterization and transfection efficiency. J. Control. Release 70, 399–421.

Mao, S.J., Hou, S.X., Zhang, L.K., Jin, H., Bi, Y.Q., Jiang, B., 2003. Prepartion of bovine serum albumin nanoparicles surface-modified with glycyrrhizin. Yao Xue Xue Bao 38, 787–790.

Mao, S.J., Hou, S.X., He, R., Zhang, L.K., Wei, D.P., Bi, Y.Q., Jin, H., 2005. Uptake of albumin nanoparticle surface modified with glycyrrhizin by primary cultured rat hepatocytes. World J. Gastroenterol. 28, 3075–3079.

Meng, W., Parker, T.L., Kallinteri, D.A., Walker, D.A., Higgins, S., Hutcheon, G.A., Garentt, M.C., 2006. Uptake and metabolism of novel biodegradable poly(glycerol-adipate) nanoparticles in DAOY monolayer. J. Control. Release 116, 314–321.

Meschini, S., Molinari, A., Calcabrini, A., Citro, G., Arancia, G., 1994. Intracellular localization of the antitumour drug adriamycin in living cultured cells: a confocal microscopy study. J. Microsc. 176, 204–210.

Musyanovych, A., Rossmanith, R., Tontsch, C., Landfester, K., 2007. Effect of hydrophilic comonomer and surfactant type on the colloidal stability and size distribution of carboxyl- and amino-functionalized polystyrene particles prepared by miniemulsion polymerization. Langmuir 23, 5367–5376.

Na, K., Bum Lee, T., Park, K.H., Shin, E.K., Lee, Y.B., Choi, H.K., 2003. Self-assembled nanoparticles of hydrophobically modified polysaccharide bearing vitamin H as a targeted anti-cancer drug delivery system. Eur. J. Pharm. Sci. 18, 165–173.

Negishi, M., Irie, A., Nagata, N., Ichikawa, A., 1991. Specific binding of glycyrrhetinic acid to the rat liver membrane. Biochim. Biophys. Acta 1066, 77–82.

Nguyen, L.T., Ishida, T., Ukitsu, S., Li, W.H., Tachibana, R., Kiwada, H., 2003. Culture time-dependent gene expression in isolated primary cultured rat hepatocytes by transfection with the cationic liposomal vector TFL-3. Biol. Pharm. Bull. 26, 880–885.

Onishi, H., Machida, Y., 1999. Biodegradation and distribution of water-soluble chitosan in mice. Biomaterials 20, 175–182.

Osaka, S., Tsuji, H., Kiwada, H., 1994. Uptake of liposomes surface modified with glycyrrhizin by primary cultured rat hepatocytes. Biol. Pharm. Bull. 17, 940–943.

Redhead, H.M., Davis, S.S., Illum, L., 2001. Drug delivery in poly(lactide-co-glycolide) nanoparticles surface modified with poloxamer 407 and poloxamine 908: in vitrocharacterisation and in vivo evaluation. J. Control. Release 70, 353–363.

Sawamura, T., Nakada, H., Hazama, H., Shiozaki, Y., Sameshima, Y., Tashiro, Y., 1984. Hyperasialoglycoproteinmia in patients with chronic liver diseases and/or liver cell carcinoma. Asialoglycoprotein receptor in cirrhosis and liver cell carcinoma. Gastroenterology 87, 1217–1221.

Stella, B., Arpicco, S., Peracchia, M.T., Desmaële, D., Hoebeke, J., Renoir, M., D'Angelo, J., Cattel, L., Couvreur, P., 2000. Design of folic acid-conjugated nanoparticles for drug targeting. J. Pharm. Sci. 89, 1452–1464.

Sudimack, J., Lee, R.J., 2000. Targeted drug delivery via the folate receptor. Adv. Drug Deliv. Rev. 41, 147–162.

Tiyaboonchai, W., Limpeanchob, N., 2007. Formulation and characterization of amphotericin B-chitosan-dextran sulfate nanoparticles. Int. J. Pharm. 329, 142–149.

Tsuji, H., Osaka, S., Kiwada, H., 1991. Targeting of liposomes surface-modified with glycyrrhizin to the liver. I. Preparation and biological disposition. Chem. Pharm. Bull. 39, 1004–1008.

Wu, Y., Yang, W., Wang, C., Hu, J., Fu, S., 2005. Chitosan nanoparticles as a novel delivery system for ammonium glycyrrhizinate. Int. J. Pharm. 295, 235–245.